Huntingtin coordinates the dynein-mediated dynamic positioning of endosomes and lysosomes

Juliane P. Caviston, Allison L. Zajac, Mariko Tokito, and Erika L.F. Holzbaur
Department of Physiology, University of Pennsylvania School of Medicine, Philadelphia, PA 19104

ABSTRACT **Huntingtin (Htt) is a membrane-associated scaffolding protein that interacts with microtubule motors as well as actin-associated adaptor molecules. We examined a role for Htt in the dynein-mediated intracellular trafficking of endosomes and lysosomes. In HeLa cells depleted of either Htt or dynein, early, recycling, and late endosomes (LE)/lysosomes all become dispersed. Despite altered organelle localization, kinetic assays indicate only minor defects in intracellular trafficking. Expression of full-length Htt is required to restore organelle localization in Htt-depleted cells, supporting a role for Htt as a scaffold that promotes functional interactions along its length. In dynein-depleted cells, LE/lysosomes accumulate in tight patches near the cortex, apparently enmeshed by cortactin-positive actin filaments; Latrunculin B-treatment disperses these patches. Peripheral LE/lysosomes in dynein-depleted cells no longer colocalize with microtubules. Htt may be required for this off-loading, as the loss of microtubule association is not seen in Htt-depleted cells or in cells depleted of both dynein and Htt. Inhibition of kinesin-1 relocalizes peripheral LE/lysosomes induced by Htt depletion but not by dynein depletion, consistent with their detachment from microtubules upon dynein knockdown. Together, these data support a model of Htt as a facilitator of dynein-mediated trafficking that may regulate the cytoskeletal association of dynamic organelles.**

Monitoring Editor
Gero Steinberg
University of Exeter

Received: Mar 18, 2010
Revised: Nov 30, 2010
Accepted: Dec 7, 2010

INTRODUCTION

Maintenance of cellular homeostasis as well as proper cell growth and function depend on effective intracellular transport. The polarized microtubule cytoskeleton provides tracks for the long-distance cytoplasmic transport of membranous organelles, whereas actin filaments are tracks for short, dispersive movements near the cell cortex (Soldati and Schliwa, 2006). Members of the kinesin superfamily move cargoes along microtubules primarily toward the cell periphery, whereas cytoplasmic dynein, with its activator dynactin, is the major minus-end–directed microtubule motor, moving cargoes toward the cell center (reviewed in Caviston and Holzbaur, 2006). Several classes of the myosin superfamily are involved in vesicle formation at the plasma membrane as well as membrane trafficking along the actin cytoskeleton; specifically, myosin VI has been implicated in delivery of endocytic cargo to the microtubule cytoskeleton (Soldati and Schliwa, 2006). Coordination of transport between the microtubule and actin cytoskeletons is essential for efficient transport of membranous organelles, such as lysosomes (Cordonnier *et al.*, 2001).

Perturbations in intracellular trafficking and transport can inhibit targeted delivery and can result in human disease (Aridor and Hannan, 2000, 2002; Dell'Angelica, 2009). Defective cytoskeletal transport in neurons, highly polarized cells with extended axonal processes, has also been linked to human disease. Growing evidence suggests that mutations in microtubule motors, and in proteins that are actively transported by microtubule motors, can induce neurodegeneration (Chevalier-Larsen and Holzbaur, 2006). Huntington's disease (HD) is a fatal neurodegenerative disease caused by a polyglutamine expansion in the protein huntingtin (Htt) (The Huntington's

This article was published online ahead of print in MBoC in Press (http://www.molbiolcell.org/cgi/doi/10.1091/mbc.E10-03-0233) on December 17, 2010.

Address correspondence to: Erika L.F. Holzbaur (holzbaur@mail.med.upenn.edu).

Abbreviations: DHC, dynein heavy chain; DIC, dynein intermediate chain; EEA1, early endosome antigen 1; EGF, epidermal growth factor; EGFR, epidermal growth factor receptor; HAP1, huntingtin-associated protein 1; HD, Huntington's Disease; Htt, huntingtin; LAMP1, LE/lysosomal-associated membrane protein 1; LE, late endosomes; p-ERK1/2, phospho-extracellular signal-regulated kinases 1 and 2; Tf, transferrin; TfR, transferrin receptor.

Disease Collaborative Research Group, 1993). The molecular mechanisms underlying the disorder and the toxic nature of mutant Htt have been widely studied, and defects in intracellular trafficking have been observed. However, the function of the normal form of Htt, which is expressed in all cells, both neuronal and nonneuronal, is less well understood (reviewed in Caviston and Holzbaur, 2009).

Htt is a 350-kDa, vesicle-associated protein (DiFiglia *et al.*, 1995) that has been localized to Golgi vesicles (del Toro *et al.*, 2009), early endosomes (Pal *et al.*, 2006), recycling endosomes (Li *et al.*, 2009), and lysosomes (Kegel *et al.*, 2005). Studies of the primary structure reveal that an N-terminal membrane association signal may target Htt to late endosomes, autophagosomes, and the endoplasmic reticulum (Atwal *et al.*, 2007); another N-terminal amino acid motif binds phospholipids enriched at the plasma membrane (Kegel *et al.*, 2005). Htt may act as a scaffold, associating with several factors involved in vesicle trafficking, such as Htt-associated protein 1 (HAP1) (Harjes and Wanker, 2003; Li and Li, 2004; Truant *et al.*, 2006; Caviston and Holzbaur, 2009). Interestingly, HAP1 has been shown to bind to kinesin-1, as well as the p150^{Glued} subunit of dynactin (Engelender *et al.*, 1997; Li *et al.*, 1998; McGuire *et al.*, 2006; Twelvetrees *et al.*, 2010). Htt itself directly binds the microtubule motor cytoplasmic dynein (Caviston *et al.*, 2007), suggesting that a complex comprised of Htt/HAP1, dynein/dynactin, and kinesin-1 assembled on vesicles may promote bidirectional transport in the cell. Immunoprecipitation experiments examining the association of endogenous proteins in brain extracts support the formation of such a complex (Caviston *et al.*, 2007). Furthermore, Htt has been shown to facilitate bidirectional motility of vesicles in vitro (Caviston *et al.*, 2007). In neurons, phosphorylation of Htt has been shown to promote plus-end–directed vesicle motility (Colin *et al.*, 2008), suggesting that Htt may act as a molecular switch to change the direction of vesicular movement along the microtubule. In addition, Htt interacts with proteins involved in actin-based transport, such as optineurin (Sahlender *et al.*, 2005), leading to the hypothesis that Htt may act as a switch to alter the cytoskeletal association of vesicles. In support of this idea, the binding of HAP40 to Htt was shown to induce a change in the affinity of early endosomes from microtubules to actin (Pal *et al.*, 2006).

Bidirectional motility is fundamental to endosomal trafficking and transport in mammalian cells. Early endosomes undergo dynein-dependent sorting and movement toward the cell center (Driskell *et al.*, 2007), and recycling endosomes export cargo to the plasma membrane, which depends on kinesin activity (Soldati and Schliwa, 2006). Thus Htt is an excellent candidate molecule to mediate the functional interplay of opposing molecular motors on endosomal cargo. In this study, we examined the localization and function of early, recycling, and late endosomes (LE)/lysosomes in the absence of Htt or dynein. Our results demonstrate that, in HeLa cells, Htt and dynein are required for the perinuclear positioning, but not function, of early endosomes, recycling endosomes, and LE/lysosomes. Interestingly, cells depleted of dynein exhibit LE/lysosomal accumulations along the cell periphery. These peripheral lysosomal patches show reduced colocalization with microtubules and instead appear to localize to regions enriched in cortactin and cortical actin. In cells depleted of Htt, LE/lysosomes were also dispersed; however, they remained colocalized with microtubules. These observations suggest that Htt may modulate organelle association with microtubules and actin. Overall, our data support a role for Htt as a regulator of dynein-mediated transport of endosomal organelles, acting as a scaffold protein to integrate motor proteins and cytoskeletal effector molecules, and consequently to coordinate organelle association with both the microtubule and actin cytoskeletons.

RESULTS

Early endosomes are dispersed in cells depleted of Htt or dynein

Endosomal trafficking and transport in mammalian cells is bidirectional, relies on an intact cellular cytoskeleton, and requires functional molecular motors. Receptors are taken up from the plasma membrane into endocytic vesicles that mature into early endosomes and undergo dynein-dependent sorting and movement toward the cell center (Driskell *et al.*, 2007). We specifically depleted cellular levels of Htt using RNAi (~80% knockdown; Figure 1B and Supplemental Figure 1, A and B) and examined the distribution of the early endosome compartment, labeled with antibody against early endosome antigen 1 (EEA1). We found that depletion of Htt leads to the dispersal of early endosomes toward the cell periphery as compared with control cells transfected with scrambled oligo (Figure 1A, left panel) or mock-treated cells (data not shown). A 3-min pulse of Alexa 594–conjugated transferrin (Tf-594) followed by a 12-min chase labels early endosomes (Pal *et al.*, 2006); the Tf-594–positive early endosomes are more peripheral in Htt-depleted cells in comparison with control cells (Figure 1A, right panel). Averaged linescans (Figure 1C) of these cells reveal that, unlike control cells, which exhibit a maximum of fluorescence intensity at the cell center, Htt RNAi cells have a much broader peak of Tf-594 fluorescence intensity, indicating a more even distribution throughout the cytoplasm. In some cells, we noted accumulation of Tf-594–positive early endosomes near the cell cortex. Early endosome mislocalization as detected by Tf-594 or endogenous EEA1 in Htt RNAi cells could be rescued by transfecting knockdown cells with a full-length mouse construct of Htt (Saudou *et al.*, 1998) resistant to our RNAi oligos (Supplemental Figure S1, C and D; and data not shown).

In comparison, knockdown of dynein heavy chain (DHC), or knockdown of p150^{Glued} (a major dynactin component), results in a more dramatic mislocalization of early endosome compartments toward the cell periphery, with the Tf-594 compartments aligning along the cell edge in most cells (Figure 1A–C and Supplemental Figure S2), similar to what has been reported in the presence of a dominant-negative inhibitor of dynein/dynactin function (Valetti *et al.*, 1999). This enhanced peripheral accumulation seen in DHC RNAi cells as compared with Htt RNAi cells suggests that depletion of Htt is not the equivalent of depleting cells of functional dynein/dynactin complex, but rather represents a decrease in efficient transport toward the cell center. These observations are consistent with a role for Htt in facilitating dynein-mediated endosome movement.

To test whether this mislocalization is correlated with a defect in uptake from the cell surface, Htt RNAi, DHC RNAi, or control RNAi cells were incubated on ice with primary antibody against Tf receptor (TfR), then shifted to 37°C to allow internalization of the antibody. The extent of internalization as a function of time was measured using flow cytometry (Figure 1D). Over time, Htt RNAi cells internalized the same percentage of total TfR as control cells, indicating no defect in the kinetics of uptake from the plasma membrane. In addition, there was no change in the kinetics of uptake in dynein-depleted cells, consistent with the results reported for cells overexpressing a dominant-negative subunit of dynactin (Valetti *et al.*, 1999). A comparison of surface-associated levels of TfR antibody at the 0 time point indicates that cells lacking Htt or dynein have higher steady-state levels of TfR on the surface (Figure 1E) compared with control cells. By Western blot, Htt RNAi cells have about a two-fold increase in total cellular levels of TfR (Figure 1B), which may explain the increase in surface levels. In contrast, there is

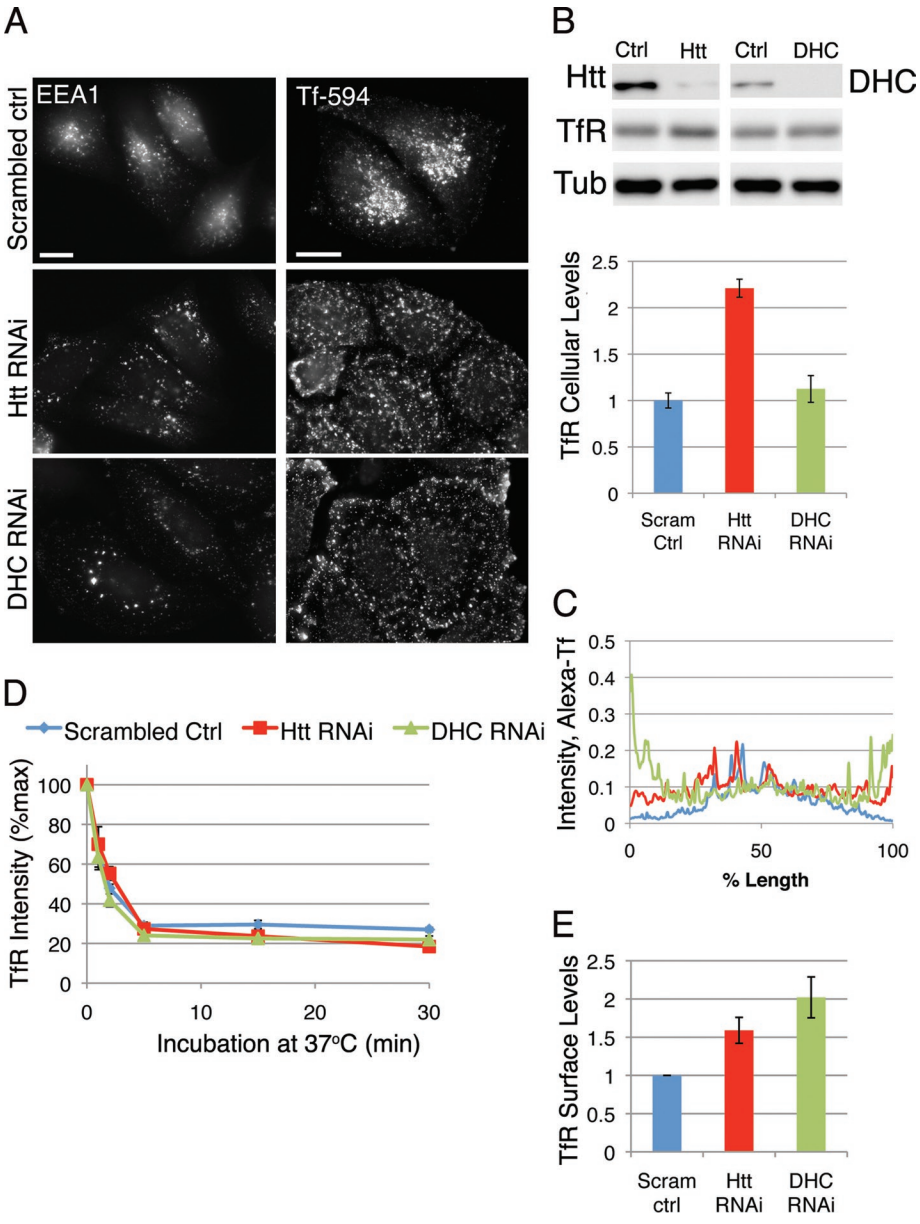

FIGURE 1: Htt is required for perinuclear early endosome positioning but not for transferrin uptake from the plasma membrane. (A) HeLa cells transfected with scrambled control oligo (top), Htt RNAi (middle), or DHC RNAi (bottom) were stained with antibodies against EEA1 (left column) or given a quick pulse-chase with 594-Alexa-Tf (right column) to label early endosomes. Scale bar = 20 μm. (B) Top: Western blot demonstrating decreased levels of Htt (top left panel) and DHC (top right panel) in RNAi cells. TfR is detected in the middle panel and tubulin is shown as a loading control. Bottom: Due to the near-saturation levels of tubulin immunoreactivity, TfR levels were normalized using β-catenin (not shown) as a loading control. (C) Linescans of control (n = 12), Htt RNAi (*n* = 11), and DHC RNAi (*n* = 12) cells pulsed with Tf-594 (see A), with average fluorescence intensity along the length of the cell. (D) Control, Htt RNAi, and DHC RNAi cells were incubated with antibody to TfR at 4°C, then shifted to 37°C to allow internalization for 0, 1, 2, 5, 15, and 30 min; incubated with fluorescent secondary antibody; then fixed and processed for flow cytometry. Average fluorescent intensity of TfR is plotted as percent of maximum (n = 4). (E) TfR present on the surface is measured as fluorescence intensity at the zero time point for scrambled control, Htt RNAi, and DHC RNAi cells, normalized by the mean intensity for scrambled control cells. Error bars, ±SEM.

no significant increase in total levels of TfR in DHC RNAi cells, suggesting that the increased surface levels are due to an isolated increase in that specific pool of receptor, perhaps because of more complete inhibition of minus-end–directed transport that occurs in the absence of dynein.

Htt and dynein are required to maintain the localization of recycling endosomes

From the early endosome, some cargoes are delivered to recycling endosomes for return to the plasma membrane. Although there was no defect in cell surface uptake, we hypothesized that the mislocalization of endosome compartments may be correlated to a recycling defect in cells lacking Htt or dynein. The distribution of endogenous Rab11, a Rab GTPase known to regulate the recycling compartment (Maxfield and McGraw, 2004), is altered in Htt RNAi and DHC RNAi cells (Figure 2A). The Rab11-positive recycling compartment is not concentrated toward the cell center in either Htt RNAi or DHC RNAi cells, in comparison with control cells (arrows). Instead, Rab11-positive organelles have a more dispersed, peripheral localization, which is especially evident in cells lacking dynein, in which Rab11 appears to accumulate in plasma membrane protrusions (Figure 2A, arrowheads).

Such dispersion of recycling organelles might be expected to disrupt the efficiency of recycling in cells depleted of Htt or dynein. To test this, we used a standard assay in which fluorescent-Tf is endocytosed and delivered back to the cell surface, and efficiency of recycling is detected by a loss of fluorescence intensity over time. Images of cells fixed throughout the time course demonstrate that, unlike control cells, compartments containing fluorescent-Tf in Htt RNAi and DHC RNAi (Figure 2B, middle and bottom rows) never accumulate at the perinuclear region. However, similar to control cells, they lose the bulk of fluorescent-Tf by 60 min. Flow cytometry confirmed that fluorescence intensity decreased at approximately the same rate for both control and Htt or dynein knockdown cells, indicating that there was no discernible defect in the kinetics of recycling (Figure 2C).

Although we saw no difference in recycling kinetics, we did note that the fluorescence intensities of both Htt knockdown and dynein knockdown cells were higher than control cells at all time points (Figure 2D). For Htt-depleted cells, this may be partly explained by the increase in cellular levels of TfR (Figure 1B). This finding is consistent with previous reports of Htt as an iron-regulated protein that functions in making endocytosed iron accessible to cells (Hilditch-Maguire *et al.*, 2000; Lumsden *et al.*, 2007). This differs from results of a recent study of fibroblasts from HD patients, which showed that, due to inhibition of nucleotide exchange on Rab11, Tf is delayed in recycling back to the plasma membrane (Li *et al.*, 2009). Although we do not see a change in kinetics of Tf trafficking under Htt RNAi conditions, it is possible that, in the presence

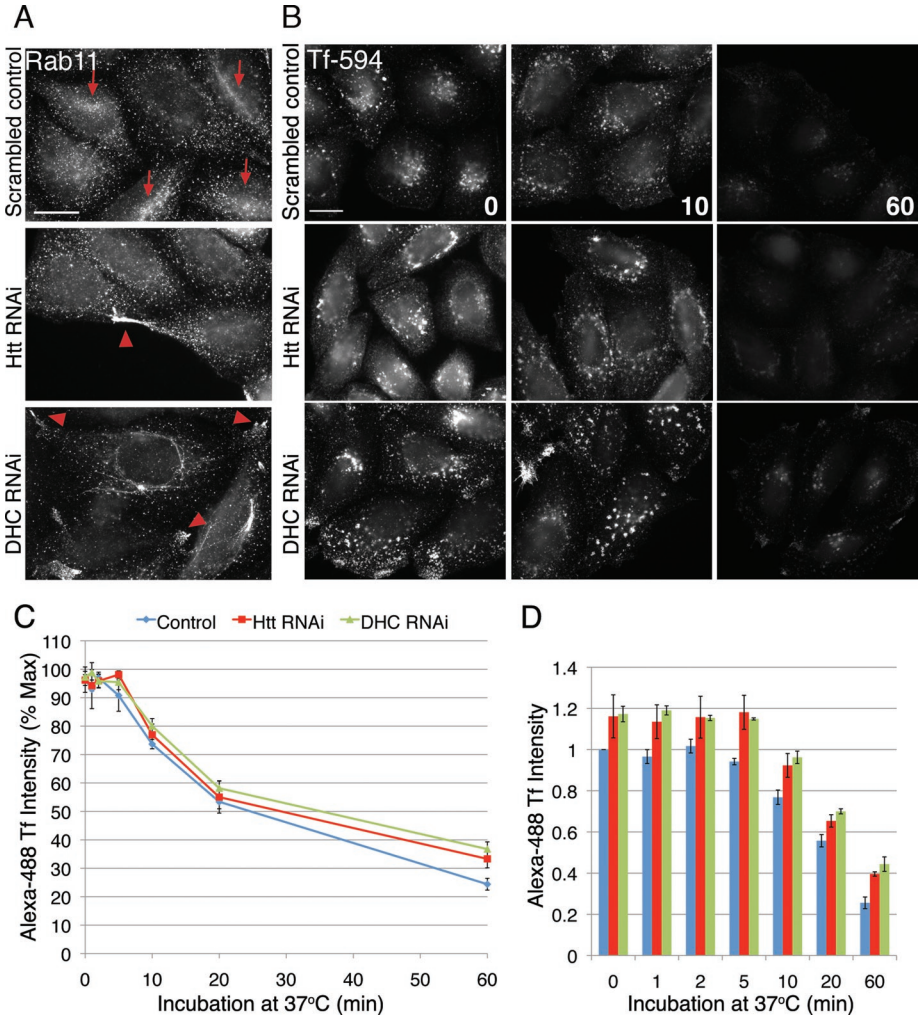

FIGURE 2: Recycling compartments in cells depleted of Htt or dynein lack perinuclear concentration, but kinetics of recycling are normal. (A) Scrambled control cells (top), Htt RNAi cells (middle), and DHC RNAi cells stained for Rab11. Concentrations of Rab11 at the perinucleus are denoted with arrows, and peripheral accumulations are denoted by arrowheads. (B) Cells were pulsed with Alexa594-Tf for 30 min to label recycling compartments, washed extensively, and then transferred to regular media and fixed at various time points. Shown are images of scrambled control (first row), Htt RNAi (second row), and DHC RNAi (third row) cells fixed at 0 (left), 10 (middle), and 60 (right) min. (C) Cells were treated as above but with Alexa 488-Tf, and cell intensities at 0, 1, 2, 5, 10, 20, and 60 min were measured by flow cytometry. Average fluorescence intensity of 488-Tf is plotted as percent of maximum. Htt RNAi, n = 3; DHC RNAi, n = 4; scrambled control, n = 7. (D) Alexa 488-Tf intensities at each time point of (C), normalized by the mean fluorescence intensity of scrambled control. All scale bars = 20 μm. Error bars, ±SEM.

of mutant Htt in the HD fibroblasts, there are other alterations, such as sequestration of other functional proteins, resulting in defective Rab11 GEF activity and subsequent problems with Tf trafficking.

We did not observe a change in total TfR levels in cells depleted of dynein (Figure 1B). Therefore, the measurable increase in fluorescent Tf on the surface of dynein-depleted cells (Figure 2D) could be strictly due to uncoupling of inward and outward vesicle trafficking, which results in more peripherally localized vesicular cargo and subsequently increased surface deposition of TfR.

Htt and dynein are required for the perinuclear positioning of LE/lysosomes

Proteins destined for the degradative pathway are sorted from the early endosome to the LE and shuttled to the lysosome for proteolysis. In addition to early and recycling endosomes, compartments that are positive for the LE/lysosome marker LAMP1 also rely on Htt for proper positioning. Unlike control cells, which have a perinuclear concentration of LE/lysosomes, cells lacking Htt exhibit dispersed LE/lysosomes and, in some cells, accumulate LE/lysosomes on the cell periphery (Figure 3A, top and middle panels, arrowheads). This LE/lysosome mislocalization was rescued by transfection of knockdown cells with full-length Htt (see Figure 4A).

As seen in previous studies (Burkhardt *et al.*, 1997; Harada *et al.*, 1998; Valetti *et al.*, 1999), cells lacking functional dynein exhibit dramatic mislocalization of LE/lysosomes, with most cells showing accumulation of lysosomes at cell protrusions (Figure 3A, bottom panel). Averaged linescans of LAMP1 immunofluorescence demonstrate that control cells display a peak of intensity toward the center of the cell, whereas Htt knockdown cells have a much broader peak, indicating that the LE/lysosomes are more evenly distributed throughout the cytoplasm; predictably, dynein knockdown cells exhibit the most dramatic mislocalization of LE/lysosomes, with the peak of LAMP1 intensity near the cell edges (Figure 3B).

We also examined the effects of Htt or dynein depletion on lysotracker-positive organelles in live cell assays. LE/lysosome dynamics in scrambled oligo-treated control cells are complex (Supplemental Video 1), consistent with both diffusional and processive aspects of motility (Hendricks *et al.*, 2010). Although some motility persists in both Htt- and dynein-depleted cells (Supplemental Videos 2 and 3, respectively), this movement is qualitatively different from controls. To quantitatively assess the differences in LE/lysosome motility in an unbiased manner, we calculated a displacement index for each condition (Quintero *et al.*, 2009; see *Materials and Methods* for details on the analysis). We found that both the Htt- and dynein-depleted cells showed a lower displacement index (3.74 ± 0.17 and 3.85 ± 0.18, respectively, given as mean ± SEM) than scramble-treated control cells (4.68 ± 0.22; group means significantly different by analysis of variance (ANOVA), $p = 0.0011$; means for Htt- and dynein-depleted cells are each significantly different from control but not significantly different from each other by Tukey's *t* test). These data are consistent with decreased lysosomal motility in both Htt- and dynein-depleted cells.

To test whether the mislocalization of LE/lysosomes affects lysosomal function, cells were stimulated with epidermal growth factor (EGF), and the degradation of EGF receptor (EGFR) and activation of downstream effectors extracellular signal–related kinase (ERK) 1/2 were measured by Western blot. In cells lacking Htt, the kinetics of EGFR degradation and ERK1/2 phosphorylation (Figure 3C–E) were approximately equal to that of control cells. Similarly, cells

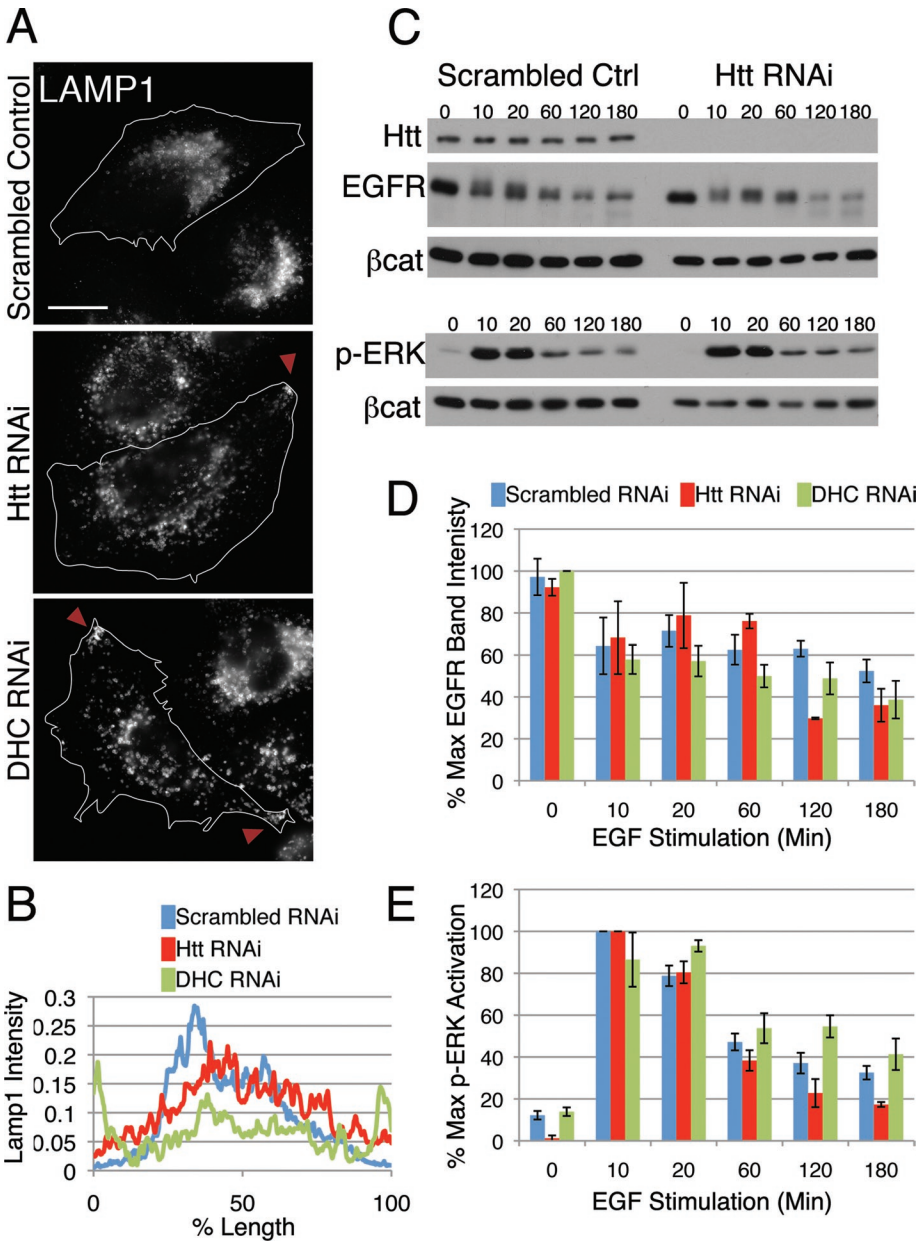

FIGURE 3: LE/lysosomes are mislocalized in Htt RNAi cells; however, degradative function is normal. (A) LE/lysosomes in scrambled control (top), Htt RNAi (middle), and DHC RNAi cells (bottom) were visualized by staining cells for LAMP1. Peripheral accumulations are denoted with arrowheads. Scale bar = 20 μm. (B) Linescans of LAMP1 intensity in scrambled control (blue; n = 13), Htt RNAi (red; n = 15), and DHC RNAi cells (green; n = 16). (C) Western blot of scrambled control and Htt RNAi cells stimulated with EGF for various times. Cell lysates were probed for Htt, EGFR, and phospho-ERK1/2 with β-catenin as a loading control. The experiment was done in triplicate; a representative image is shown. (D, E) Densitometry of EGFR bands (D) and p-ERK1/2 bands (E) in scrambled control, Htt RNAi, and DHC RNAi cell lysates throughout the EGF stimulation, normalized for loading with β-catenin. EGF stimulation of DHC RNAi cells was performed three times in duplicate. Error bars, ±SEM.

lacking dynein also did not exhibit pronounced defects in either receptor degradation or attenuation of cell signaling (Figure 3, D and E). This indicates that Htt, like dynein, is required for proper spatial organization of LE/lysosomes in HeLa cells but is nonessential for degradative function. We did not see an inhibition of EGFR degradation similar to that seen previously in a study using a dominant-negative approach to block dynein function (Taub *et al.*, 2007). The discrepancy may reflect the difference in the techniques between overexpressing a dominant-negative construct versus depletion of endogenous protein by RNAi.

Full-length Htt is essential to rescue organelle positioning defects

To confirm that the disruption of early and LE/lysosomes is indeed due to the loss of Htt, we transfected knockdown cells with a full-length mouse construct of Htt (Saudou *et al.*, 1998) resistant to our RNAi oligos. As shown in Supplemental Figure S1, the perinuclear localization of early endosomes was restored by expression of this construct. Likewise, LE/lysosomes were concentrated toward the cell center in Htt RNAi cells rescued with full-length Htt (Figure 4A). Next we tested Htt truncation constructs for their ability to rescue organelle positioning (Figure 4B). In a recent report, a truncation construct of Htt consisting of amino acids (aa) 1–480 (Htt480) increased the velocity of bidirectional motility of post–Golgi vesicles in neuronal cells (Colin *et al.*, 2008), suggesting that expression of Htt480 might be sufficient to rescue the defects of organelle localization seen in Htt-depleted cells. Thus we transfected control and Htt-depleted cells either with Htt480, which lacks a dynein-binding site that has been mapped to residues aa601–698 of Htt (Caviston *et al.*, 2007), or with a longer construct of mouse Htt spanning residues aa1–1472 (Htt1472) (Figure 4C), that contains the dynein-binding site and a greater portion of the HEAT repeat-rich region (aa90–3144) that is predicted to mediate protein–protein interactions (MacDonald, 2003).

To assess whether the expression levels of transfected Htt constructs had any effect on the perinuclear localization of LE/lysosomes, transfected cells were categorized as low/medium expressors (low/med) or high expressors (high) (see *Materials and Methods*). Introduction of exogenous Htt constructs had no effect on the localization of LE/lysosomes in control cells. Even at high levels of expression, 80–90% of cells transfected with no DNA, Htt480, Htt1472, or full-length Htt had perinuclear LE/lysosomes (Figure 4C, "Scrambled control" columns).

In contrast, expression of exogenous Htt had a dramatic effect on Htt RNAi cells (Figure 4C, "Htt RNAi") with pronounced dosage dependence. Compared with Htt-depleted cells ("no DNA"), which generally exhibit widely dispersed LE/lysosomes (only 14 ± 4% of cells had perinuclear LE/lysosomes), cells transfected with Htt480 at low/medium levels showed no changes in LE/lysosome positioning. However, at high levels, Htt480 increased the proportion of perinuclear LE/lysosomes to 30 ± 10%, and the percentage of cells with cortical patches was reduced to 9 ± 6%. Likewise, raising the expression of Htt1472 from

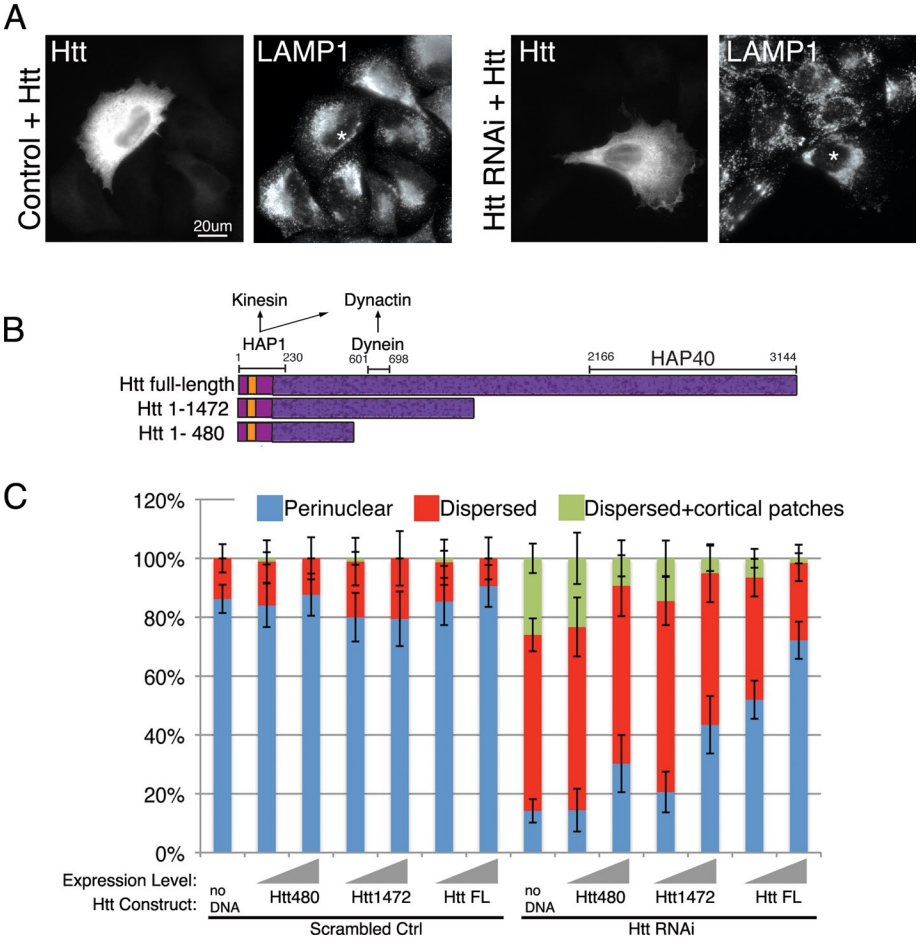

FIGURE 4: Full-length Htt is required for perinuclear organelle positioning. (A) Scrambled control (left) or Htt RNAi cells (right) were transfected with full-length Htt and stained for Htt to identify transfected cells and LAMP1. Asterisks identify transfected cells in LAMP1 panels. Scale bar = 20 µm. (C) Schematic of Htt full-length, Htt aa1–1472, and Htt aa1–480. The polyglutamine repeat region begins at aa17 (orange), and there are 36 predicted HEAT repeats spanning the length of the peptide (dark purple speckled). HAP1, which associates with kinesin and dynactin, binds to the Htt N terminus, dynein binds aa601–698, and HAP40 binding site resides at the C terminus. (D) Scrambled control (left side) or Htt RNAi (right side) cells transfected with no DNA, Htt1–480, Htt1–1472, or Htt full-length (Htt FL) were scored for perinuclear (blue), dispersed (red), or dispersed with additional cortical accumulations of LE/lysosomes (green), visualized by staining for LAMP1. To illustrate the change in phenotypes at different Htt construct expression levels, the transfected cells were binned into low or medium expressors vs. high expressors; expression level is signified by the gray ramp; n ≥ 64 cells for each condition. Error bars, ±95% CI.

low/medium to high levels further increased the proportion of cells with perinuclear LE/lysosomes to 43 ± 10% and decreased the amount of cells with cortical patches to 5 ± 4%. Finally, transfecting cells with full-length Htt had the most dramatic effect of all, increasing the proportion of cells with perinuclear LE/lysosomes to 72 ± 6% at high levels and reducing the percentage of cells with cortical patches to 2 ± 2%. Taken together, we see that addition of truncated Htt constructs did not fully rescue the perinuclear localization of LE/lysosomes. Htt480 and Htt1472, at high levels, only partially restored the perinuclear LE/lysosomal concentration. Full-length Htt more completely restored LE/lysosomal localization to the perinuclear region.

Htt may facilitate a switch in the cytoskeletal association of lysosomes

We examined the association of peripheral LE/lysosomal patches formed by depletion of either dynein or Htt with the microtubule and actin cytoskeletons. First, we determined that depletion of either dynein or Htt had no marked effect on the organization of the microtubule cytoskeleton (Figure 5) or on microtubule dynamics as assessed by monitoring EB1 comet tails in live cell assays (means of EB1-comet tail velocity are not significantly different by one-way ANOVA, n = 50 cells per condition). Htt depletion also had no marked effect on actin filament organization as assessed by phalloidin staining (Figure 6). Depletion of dynein did induce an increase in stress fibers (Figure 6B), as previously noted (Loubery *et al.*, 2008). Dynein-depleted cells were usually somewhat larger and flatter than either control or Htt-depleted cells, as well.

When we compared the distribution of peripheral LE/lysosomal patches with the microtubule cytoskeleton, we found that, in cells depleted of dynein, the LE/lysosomal patches were localized near the ends of microtubules, but no longer colocalized with these cytoskeletal tracks (Figure 5, B and C). LE/lysosomes in these patches show an 8.6 ± 2.1% (±SEM, n = 17) colocalization with microtubules, significantly ($p = 0.0015$) lower than the 42 ± 18% (n = 4) colocalization measured in the very rare peripheral patches observed in mock-treated control cells (Figure 5, A and G). This decrease in association of peripheral LE/lysosomes with microtubules was not seen in Htt-depleted cells, where the measured percent colocalization of 39.1 ± 8.9% (±SEM, *n* = 4) was not significantly different than that seen in mock-treated control cells (Figure 5, D, E, and G).

To further define the role of Htt in mediating lysosomal association with microtubules, we performed a double knockdown of dynein and Htt (Supplemental Figure S4). In these dynein- and Htt-depleted cells, we noted that peripheral LE/lysosomes remain associated with microtubules, as shown in Figure 5F. The colocalization of peripheral LE/lysosomes with microtubules was determined to be 33.0 ± 4.0% (±SEM, n = 16). This extent of colocalization is statistically different from that found for cells depleted of dynein only ($p < 0.0001$) but is not significantly different from controls. Thus the decreased association of LE/lysosomes with microtubules observed in dynein-depleted cells is rescued when Htt is also depleted, suggesting that Htt is required for disassociation of these organelles from the microtubule cytoskeleton.

We next examined the association of peripheral LE/lysosomes with actin filaments. Neither depletion of dynein nor Htt affected the colocalization of peripheral lysosomal patches with phalloidin-stained F-actin (Figure 6). However, phalloidin staining preferentially highlights stress fibers rather than dynamic actin filaments. Therefore, we also stained dynein-depleted, Htt-depleted, and control cells with antibodies to either cortactin (Figure 7A) or Arp2/3 (data not shown) as a marker for newly polymerized actin filaments (Uruno *et al.*, 2001). Htt-depleted cells showed qualitatively less

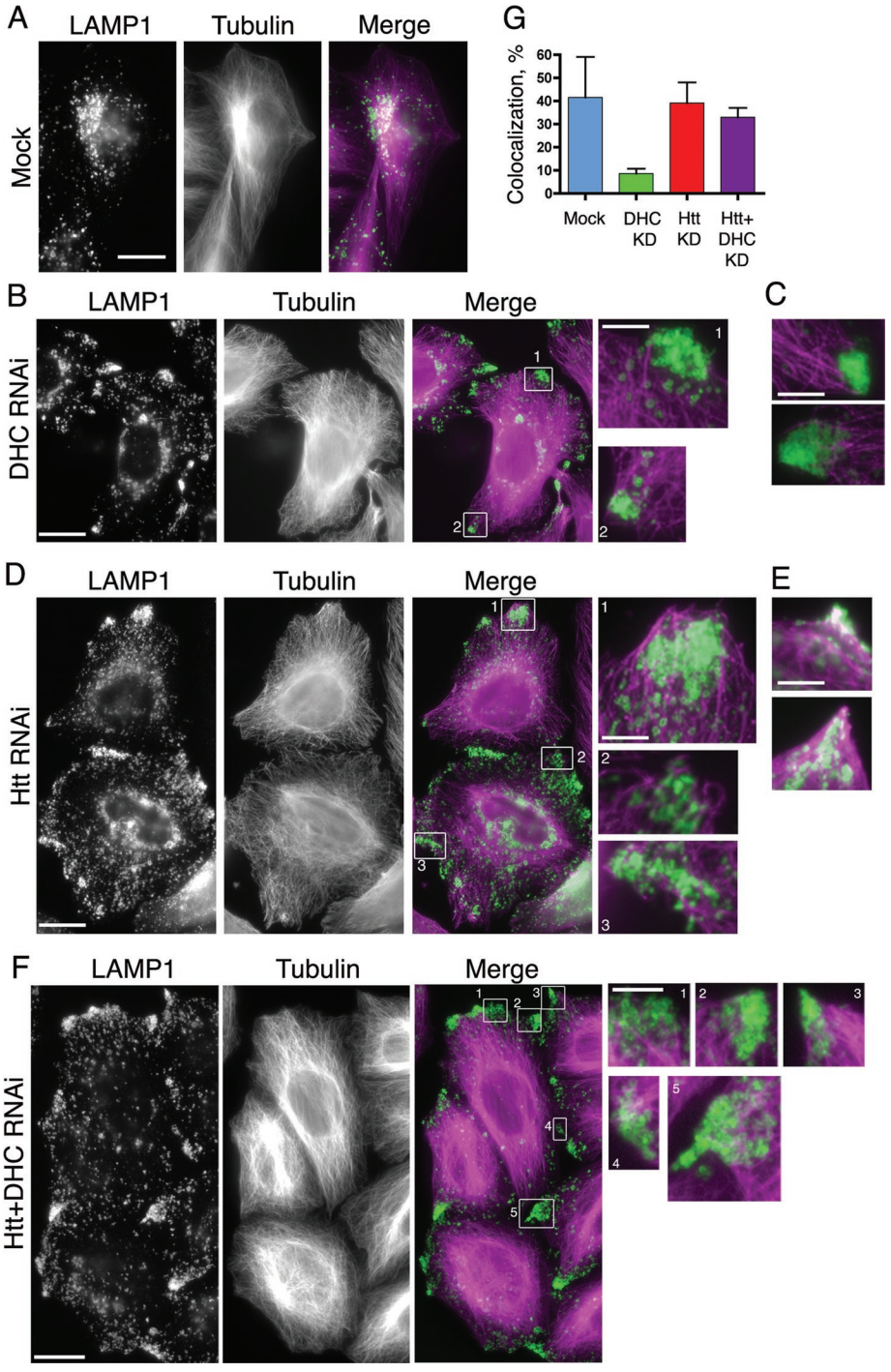

FIGURE 5: Htt may play a role in coordinating organelle association with microtubules. HeLa cells were mock transfected (A) or depleted of DHC (B) and stained for LE/lysosomes (LAMP1) and microtubules. The magnified boxed regions (boxes 1 and 2) show that the peripheral LE/lysosomes are most often found just beyond the tips of the microtubules at the cell periphery. (C) Additional merged images (as in B) featuring magnified regions of peripheral LE/lysosomes and microtubules. (D) HeLa cells depleted of Htt were stained as in (A). The magnified boxed regions (boxes 1–3) show that the peripheral LE/lysosomes are most often found enmeshed in regions dense with microtubules. (E) Additional merged images (as in D) featuring magnified regions of overlapping LE/lysosomes and microtubules at the cell edge. (F) HeLa cells depleted of Htt and dynein were stained as in (A). The magnified boxed regions (boxes 1–4) show that the peripheral LE/lysosomes are most often found enmeshed in regions dense with microtubules, similar to (D). Scale bar = 20 μm, except magnified images. The magnified images are 4× the size of original image; scale bar = 5 μm. (G) Colocalization of peripheral patches of LE/lysosomes and microtubules was quantified in mock (n = 4), DHC RNAi (n = 17), Htt RNAi (n = 4), and Htt and DHC double-knockdown cells (n = 16). Error bars, ±SEM.

overall filamentous staining with either antibody (Figure 7A, second row; and data not shown), although Western blot analysis indicates that depletion of Htt does not alter cellular levels of cortactin (data not shown). The overall colocalization of cortactin with LE/lysosomes in dynein-depleted versus mock-treated cells is not significantly different than controls (9.3 ± 2.5% vs. 10.0 ± 1.3%), but this colocalization increased dramatically if we focused on peripheral LE/lysosomal patches induced by dynein depletion (32 ± 3.4%, n = 24).

We observed that a cortactin-positive actin meshwork appears to surround the peripheral LE/lysosomal patches in dynein-depleted cells; this apparent enmeshing was absent in Htt-depleted or in Htt and dynein–double-knockdown cells (Figure 7A, compare boxes 1–4). This observation can be correlated to the overall morphology of the peripheral LE/lysosome patches, which differed significantly among the knockdown cells (Figure 7B). In dynein-depleted cells, peripheral LE/lysosomes were tightly localized into relatively small dense patches with a mean size of 36.9 ± 4.1 μm^2 (±SEM, n = 37). Peripheral patches occur much less frequently in Htt-depleted cells, are less dense (lower overall fluorescence intensity with anti-LAMP1 antibodies), and smaller 12.7 ± 4.0 μm^2 (±SEM, n = 7), similar in size to the very rare peripheral patches seen in control cells of 5.1 ± 1.0 μm^2 (±SEM, n = 4). In cells depleted for both dynein and Htt, we observed the formation of prominent peripheral patches of LE/lysosomes; these patches are both larger (62.3 ± 7.6 μm^2, ±SEM, n = 37) and less dense than the patches formed in cells depleted of dynein only. These observations suggest that a dynamic actin network may surround the peripheral LE/lysosomal patches induced by dynein depletion and that this enmeshing could increase the density of the cortical patches observed in dynein-depleted cells. In the Htt and dynein–double-knockdown cells, the patches may lack an associated actin meshwork, leading to the larger and more diffuse appearance of peripheral patches.

To test the hypothesis that an actin meshwork is associated with peripheral lysosomal patches in dynein-depleted cells, we treated control, Htt-depleted, and dynein-depleted cells with Latrunculin B to depolymerize actin filaments. Phalloidin staining of the drug-treated cells shows a loss of filamentous actin in comparison with dimethyl sulfoxide (DMSO)-treated controls (Figure 8). In DMSO-treated, dynein-depleted cells, there are prominent LAMP1-positive peripheral lysosomal patches. Latrunculin treatment leads to

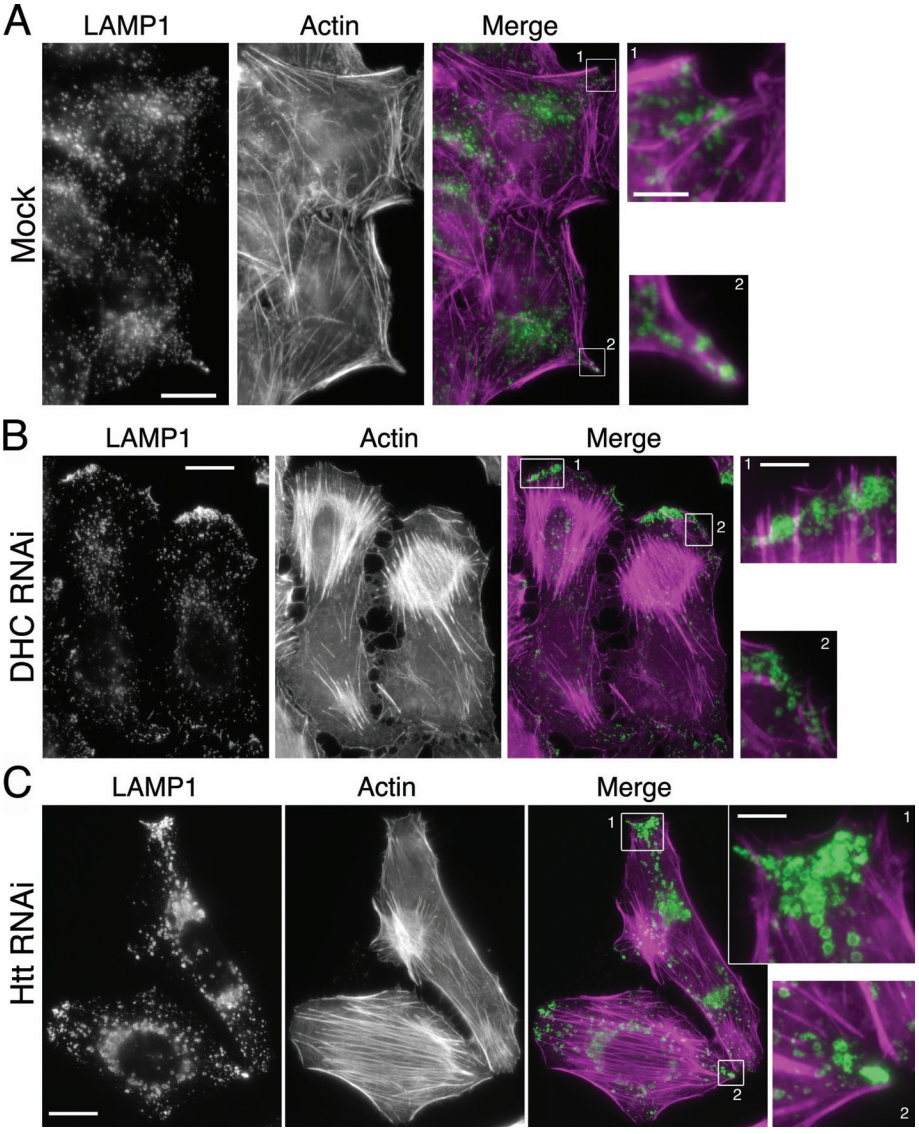

FIGURE 6: Peripheral lysosomes are distributed in regions enriched for cortical actin in cells depleted for dynein. (A) Mock-treated control cells were stained with antibody to LAMP-1 to visualize LE/lysosomes and with phalloidin to visualize F-actin. Boxed regions 1–2 highlight very tiny patches of peripheral LE/lysosomes. (B) DHC RNAi cells were stained for LE/ lysosomes (LAMP1) and F-actin. Boxed regions (1 and 2) in the merged image show that lysosomal accumulations on the cell periphery (green) are present in regions enriched with cortical actin (magenta). (C) Htt RNAi cells were stained as in (B). Boxed regions (1 and 2) in the merged image show that lysosomal accumulations on the cell periphery (green) are in areas with less marked staining for F-actin (magenta). Scale bar = 20 μm, except magnified images. The magnified images are 4× the size of original image; scale bar = 5 μm.

a quantitative loss of these peripheral patches; after 30 min in Latrunculin B, we measured a 1.8-fold decrease in the number of peripheral lysosomal patches per cell (n = 50 cells per condition). LE/lysosomes also become somewhat more centrally localized in Htt-depleted cells treated with Latrunculin B in comparison with DMSO-treated control cells (Figure 8), but Latrunculin B-treatment did not reduce the number of peripheral patches observed (n = 50 cells per condition).

LE/lysosomal dispersion in Htt-depleted but not dynein-depleted cells is mitigated by disruption of kinesin-1 activity

Four lines of evidence, detailed above, suggest that there is a switch in the cytoskeletal association of LE/lysosomes from microtubules to the actin-rich cortex under dynein-depletion conditions that is not seen in the absence of Htt: (1) an increased number of peripheral LE/lysosomal patches in dynein-depleted cells (Figure 3, A and B); (2) decreased colocalization of peripheral LE/lysosomes with microtubules in dynein-depleted cells as compared with Htt-depleted or doubly depleted cells (Figure 5); (3) enhanced cortactin staining near peripheral LE/lysosomes in dynein-depleted cells compared with Htt-depleted and Htt and dynein–double-knockdown cells (Figure 7); and (4) loss of peripheral LE/lysosomal patches in cells depleted of dynein, but not in cells depleted of Htt, induced by drug treatment to deploymerize actin (Figure 8).

If peripheral LE/lysosomes do indeed switch from an association with microtubules to an association with actin filaments in dynein-depleted cells, but not in Htt-depleted cells, then inhibiting plus-end microtubule motors driving lysosomal motility should have no affect on dynein-depleted cells; conversely, it should rescue the peripheral localization of lysosomes in Htt-depleted cells. Both kinesin-1 and kinesin-2 motors have been implicated in the anterograde transport of lysosomes (Brown *et al.*, 2005; Loubery *et al.*, 2008; Hendricks *et al.*, 2010), so we tested dominant-negative constructs to either motor for their effects on lysosomal positioning. In agreement with Brown *et al.*, we found that a headless kinesin-2 construct that functions as a dominant negative has some effect on LE/lysosomal positioning in 25–35% of transfected cells (data not shown). However, we found that inhibition of kinesin-1 in HeLa cells with a GFP-tagged construct containing kinesin-1 tail domain, GFP-KIF5C tail, which disrupts plus-end–directed kinesin-1 isoforms KIF5A, -B, and -C (Konishi and Setou, 2009), had a more significant effect on LE/lysosomal positioning, resulting in a compact perinuclear concentration of LE/lysosomes in 52 ± 8% of transfected cells (±95% CI, n = 149) (Figure 9, A and D). Transfection of cells with GFP-KIF5C stalk served as a negative control, as it has been shown to have no effect on kinesin function (Konishi and Setou, 2009) and did not change the appearance of LE/lysosomes in control cells (Figure 9A). We also examined the effects of simultaneously inhibiting kinesin-1 and kinesin-2 on LE/lysosome position by coexpressing the two dominant-negative constructs. This coexpression appeared to be cytotoxic, as judged by very low cotransfection efficiency as compared with GFP–control cotransfections as well as by the increased number of rounded and detached cells. However, tighter perinuclear clustering of LE/lysosomes was observed in some surviving cells relative to control cells (data not shown), consistent with a role for both kinesin-1 and kinesin-2 in driving the anterograde movement of these organelles.

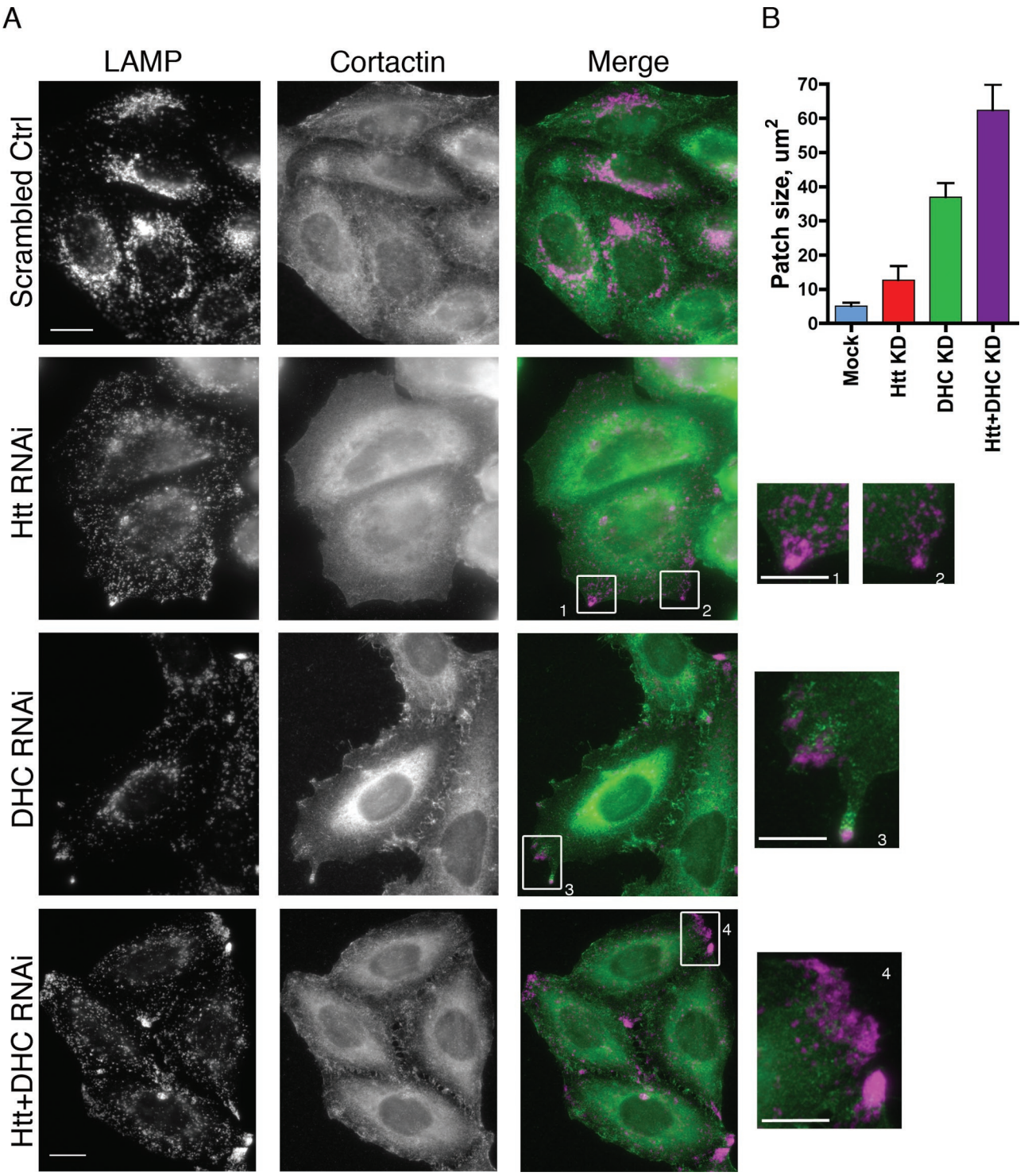

FIGURE 7: A dynamic actin network surrounds LE/lysosomes on cell periphery in dynein-depleted cells, but not Htt-depleted cells. (A) Cells transfected with control RNAi oligos (top row) and cells depleted of Htt (second row), DHC (third row), or Htt and DHC double-knockdown cells were stained for LAMP1 (first column) or cortactin (middle column). Boxes 1–4 are magnified regions highlighting the cortactin meshwork surrounding the peripheral LE/lysosomes in DHC RNAi cells, which is absent in Htt RNAi or Htt and DHC double-knockdown cells. Scale bar = 20 μm, except magnified images. The magnified images are 4× the size of original image; scale bar = 5 μm. (B) The sizes of the peripheral LE/lysosomal patches were evaluated in mock (n = 4), Htt RNAi (n = 7), DHC RNAi (n = 37), or Htt and DHC double-knockdown cells (n = 37). Error bars, ±SEM.

As inhibition of kinesin-1 had a more pronounced effect on lysosomal position, and because kinesin-1 but not kinesin-2 is known to interact with Htt via the HAP1 adaptor (McGuire *et al.*, 2006; Twelvetrees *et al.*, 2010), we chose to focus on modulating kinesin-1 function in Htt- and dynein-depleted cells. In Htt RNAi cells, there is a significant increase ($p \leq 0.0001$) in the amount of cells with

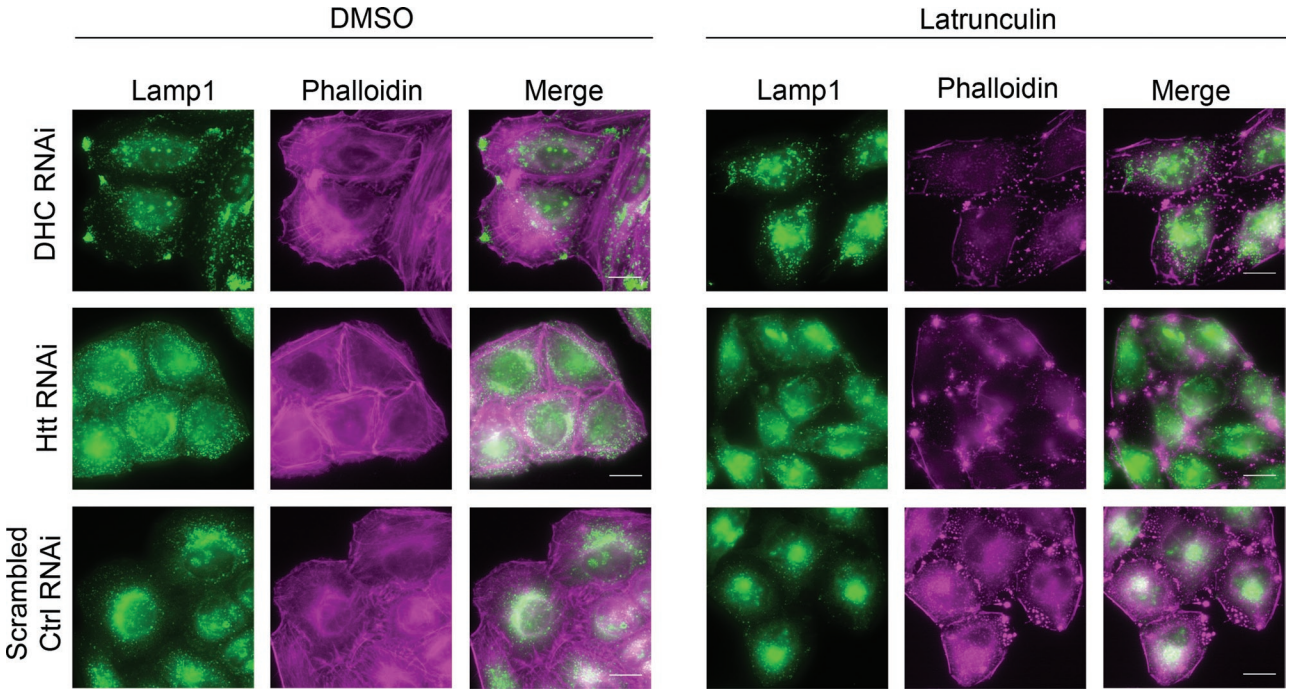

FIGURE 8: Peripheral LE/lysosomal patches induced by dynein depletion are lost upon depolymerization of actin filaments with Latrunculin B. Cells were depleted of either dynein or Htt by siRNA, or were treated with scrambled control oligos, then were treated with either DMSO (left) or Latrunculin B. Prominent peripheral LAMP1-positive patches formed in dynein RNAi cells are not seen in drug-treated cells. Latrunculin-induced depolymerization of actin filaments was visualized with phalloidin staining. Scale bar = 20 μm.

a perinuclear concentration of LE/lysosomes, from 10 ± 6% (±95% CI, n = 106) in cells transfected with the control plasmid, GFP-stalk, to 39 ± 9% (±95% CI, n = 110) transfected with GFP-tail. In addition, there is a significant decrease in the amount of cells with cortical accumulations of LE/lysosomes ($p \leq 0.0001$), from 27 ± 8% in cells transfected with GFP-stalk, to 4 ± 4% in cells transfected with GFP-tail (Figure 9, B and D). The fact that kinesin-1 inhibition dampened the severity of the LE/lysosomal dispersion exhibited by cells lacking Htt suggests that these mislocalized LE/lysosomes remain associated with microtubules and are subject to kinesin-1-mediated motility.

In striking contrast, LE/lysosomal localization in DHC RNAi cells was not significantly altered by the expression of the dominant-negative kinesin-1 construct (Figure 9, C and D). These cells continue to exhibit peripheral LE/lysosomes, despite the expression of the function-blocking tail of kinesin-1. One possibility is that the continued localization of LE/lysosomes to the periphery might be explained by the experimental method since the RNAi transfection is performed 24 h prior to the DNA transfection, leaving time for the LE/lysosomes to accumulate on the cell edge before kinesin-1 activity is decreased by addition of the tail construct. To address this issue, we cotransfected cells simultaneously with GFP-KIF5C tail and either mCherry-CC1 (Supplemental Figure S4) or FLAG-p50 (data not shown), both of which are dominant-negative constructs of dynactin subunits that effectively inhibit dynein/dynactin function. LE/lysosome localization in these double transfectants remained peripheral despite inhibition of kinesin-1 function, potentially due to continued kinesin-2 activity and/or association with cortical actin.

DISCUSSION

A recently proposed model of Htt function postulates that Htt acts as a scaffold to integrate the molecular motors and effector molecules involved in intracellular transport, acting to coordinate bidirectional vesicle motility along the microtubule and actin cytoskeletons (Caviston and Holzbaur, 2009). To delineate the specificity of Htt as a facilitator of vesicle transport, we compared the effects of Htt- and dynein-depletion on endosomal trafficking. Our results indicate that Htt acts on several populations of organelles, including early, recycling, and LE/lysosomes, to coordinate dynein-dependent positioning toward the cell center. Depletion of either Htt or dynein results in a dispersion of both endosomes and LE/lysosomes throughout the cytoplasm.

The mislocalization of both early and late endosomes we observed upon dynein depletion is consistent with previous observations (Valetti *et al.*, 1999; Driskell *et al.*, 2007; Traer *et al.*, 2007; Palmer *et al.*, 2009). Although disruption of dynein function by dominant-negative approaches has been shown to retard the efficient recycling of transferrin (Driskell *et al.*, 2007) and EGFR degradation (Taub *et al.*, 2007), we did not observe any significant defects in the kinetics of transferrin uptake and recycling, or in the kinetics of EGF receptor degradation in dynein-depleted cells. Similarly, Htt has been implicated in multiple steps in endocytosis and trafficking (reviewed in Caviston and Holzbaur, 2009). Here we show that expression of Htt is required for the normal localization of multiple endocytic compartments. However, depletion of Htt did not induce measurable defects in the kinetics of transferrin uptake or recycling or in EGFR degradation. Thus in HeLa cells, organelle mislocalization does not appear to markedly affect function.

Does Htt coordinate oppositely directed microtubule motors?

In regard to organelle localization, our observations are consistent with a model in which Htt facilitates the dynein-mediated transport of intracellular organelles. However, Htt has also been proposed as a potential regulator of kinesin-motility via HAP1 binding (McGuire *et al.*, 2006; Twelvetrees *et al.*, 2010) or phosphorylation (Colin *et al.*, 2008). Here we designed experiments to address the ability of Htt to modulate kinesin-1 function. Our results suggest that, whereas

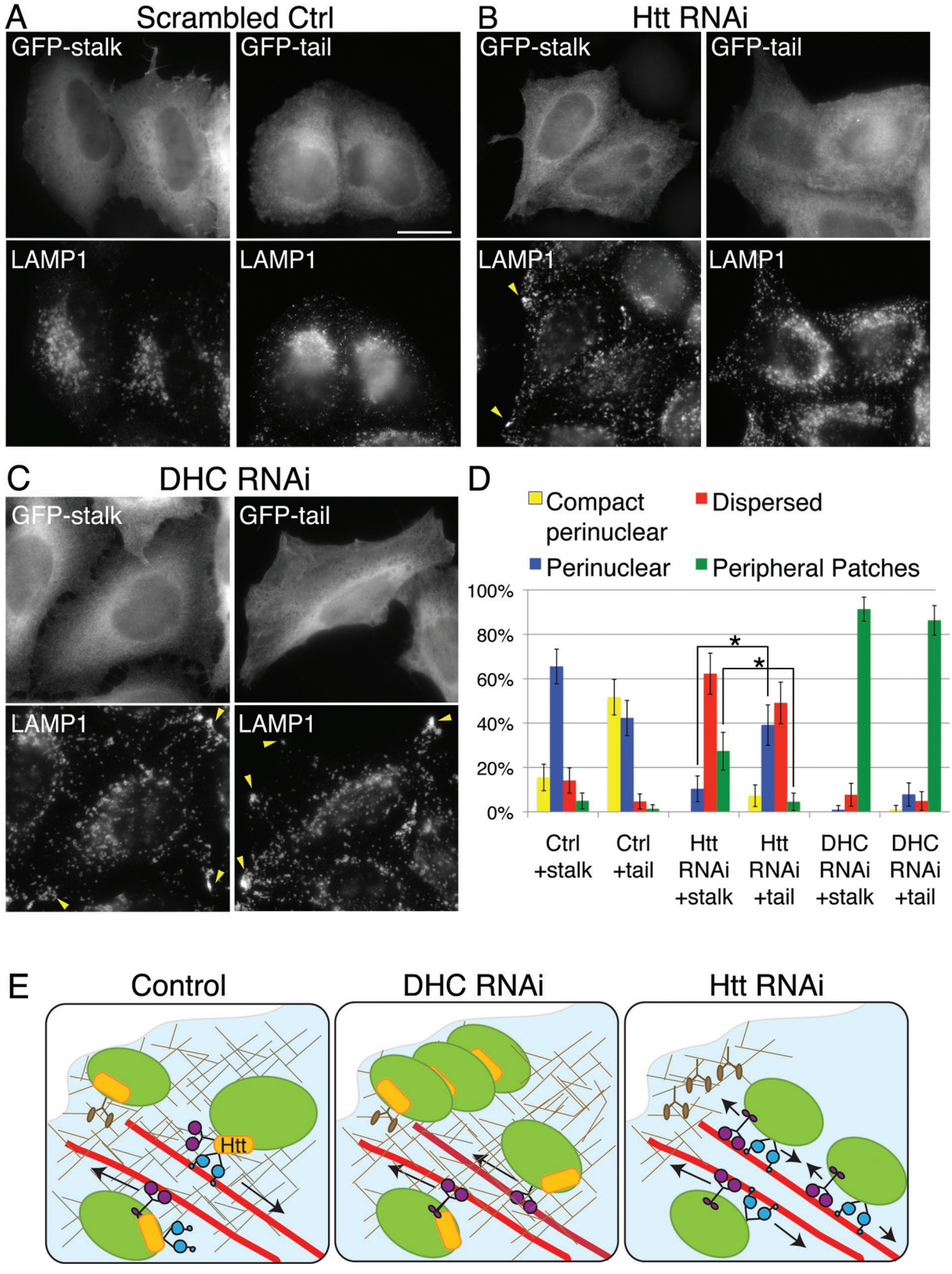

FIGURE 9: LE/lysosomal dispersion in Htt knockdown cells is mitigated by disruption of kinesin activity in Htt-knockdown but not DHC-knockdown cells. (A–C) Scrambled control (A), Htt RNAi (B), or DHC RNAi (C) cells were transfected with GFP-KIF5C stalk (GFP-stalk, left panel) or GFP-KIF5C tail (GFP-tail, right panel). LE/lysosomes of transfected cells were visualized by staining for LAMP1. Note that, in (B), transfection of GFP-tail restores a perinuclear concentration of LE/lysosomes that is absent in cells transfected with the control plasmid, GFP-stalk. In (C), peripheral accumulations of LE/lysosomes (arrowheads) persist in DHC RNAi cells in GFP-tail–positive cells. Scale bar = 20 μm.

Htt appears to strongly potentiate dynein function, kinesin-1-based transport does not appear to be seriously affected by loss of Htt in our assays. Whereas Htt interacts directly with dynein (Caviston *et al.*, 2007), the interaction with kinesin-1 is indirect, mediated by HAP-1 (McGuire *et al.*, 2006; Twelvetrees *et al.*, 2010). Thus Htt may function primarily as a dynein effector in organelle trafficking.

We also conducted a structure–function analysis to examine the contribution of different Htt domains to the rescue of organelle dispersion induced by depletion of Htt. Colin *et al.* reported that the truncated construct Htt480, which contains the binding site for the kinesin-interacting protein, HAP1 (aa1–230), and a phosphorylation site (S421) that promotes plus-end–directed motility, increased the velocity of bidirectional motility of post-Golgi vesicles in neuronal cells (Colin *et al.*, 2008). Considering this, we initially hypothesized that Htt480 might rescue organelle mislocalization in Htt RNAi cells; however, this truncated construct was not sufficient for rescue in our assays. One possible explanation is that the effect on motility seen by Colin *et al.* is specific to post-Golgi vesicles, which are expected to move primarily in the anterograde direction. Expression of Htt1472, which contains both the HAP-1 (aa1–230) and the dynein (aa601–698) binding sites, did partially reduce the mislocalization of LE/lysosomes in Htt RNAi cells, but full-length Htt was required for more complete rescue. These results suggest that full-length Htt, a scaffold that makes essential protein–protein interactions along its length, is crucial to coordinate dynein-mediated transport and maintenance of the perinuclear localization of organelles.

Htt coordinates organelle positioning and transport along the cytoskeleton

Htt has been proposed to play a role in coordinating actin and microtubule-based vesicular transport (Pal *et al.*, 2006). We found that, in cells depleted of dynein, LE/lysosomes accumulated near the cell periphery in tightly packed clusters, similar to the observations of (Loubery *et al.*, 2008); further, these LE/lysosomes were clustered in regions enriched for cortactin and Arp2/3. Lysosomes in these peripheral patches no longer colocalized with microtubules, but instead became apparently enmeshed in cortactin-positive actin filaments (Figure 9E). Consistent with this possibility, peripheral patches were reduced by actin depolymerization induced by Latrunculin B. In contrast, in cells depleted of Htt, LE/lysosomes remained associated with microtubules (Figure 9E); continued association of LE/lysosomes with microtubules was also observed in cells depleted of both Htt and dynein.

In the absence of dynein, LE/lysosomes may be more likely to bind to actin than to undergo minus-end–directed microtubule motility, perhaps because there is a decrease in vesicle-associated dynein to compete with myosin, as was recently modeled in vitro (Schroeder *et al.*, 2010). However, our results suggest that, in cells, Htt may be required to facilitate a switch in cytoskeletal tracks. The apparent off-loading of LE/lysosomes from the microtubule seen upon dynein depletion was not seen in cells doubly depleted for dynein and Htt. Consistent with this interpretation, Htt has been shown to interact with the myosin linker optineurin (Sahlender *et al.*, 2005), and the Htt-HAP40 complex has been shown to induce a switch in affinity of endosomes from microtubules to actin (Pal *et al.*, 2006).

However, our findings do not distinguish between this cytoskeletal switching model and a second model in which Htt acts as a recruitment factor for proteins like N-WASP or p61Hck, that induce the polymerization of new actin filaments (Taunton *et al.*, 2000; Vincent *et al.*, 2007). This recruitment could then result in the formation of an actin meshwork that encages peripheral LE/lysosomes, an activity that is absent in Htt-depleted cells. The observation that cortactin, a marker for newly polymerized actin, is enriched in regions surrounding peripheral LE/lysosomes in dynein-depleted, but not in Htt-depleted cells, provides support for this enmeshment model. Because Htt has scaffolding activity and the ability to integrate multiple factors involved in microtubule and actin-based transport as well as cytoskeletal remodeling, both models are consistent with a role for Htt as a coordinator of the cytoskeletal association of vesicular cargo.

Htt and the spatial regulation of intracellular trafficking

In our studies in HeLa cells, we have observed that, surprisingly, strict perinuclear localization is not required for normal recycling kinetics of transferrin uptake or recycling or for the degradation of EGFR. Although Htt may play an important role in the regulation of the cytoskeletal association of organelles in vivo, this role may be dispensable in HeLa cells. Small, nonpolarized cells may not require precise positioning of endosomes and lysosomes for proper trafficking. Spatial regulation of organelles in cells grown in culture has been previously shown to be nonessential for function: when microtubules are depolymerized, the Golgi becomes mislocalized but remains functional (Cole *et al.*, 1996).

In contrast, neuronal cells rely on a polarized cell morphology and tightly regulated transport. Therefore, it is likely that Htt plays a more essential role in facilitating dynein-mediated endosomal transport and vesicle trafficking along the cellular cytoskeleton. A role for Htt in transport in neuronal cells has been established both by studying the mutant form of Htt that causes HD and by depleting endogenous Htt. Either expression of mutant Htt or depletion of endogenous Htt causes defects in the transport of mitochondria, BDNF, and APP (Gauthier *et al.*, 2004; Trushina *et al.*, 2004; Her and Goldstein, 2008), suggesting that some trafficking and transport defects that occur in the presence of mutant Htt could be due to a loss of wild-type function induced by the expansion of polyglutamine repeats. Further elucidation of the function of normal Htt is thus necessary in order to better understand the dysfunctional nature of mutant Htt and the pathogenesis of HD.

(D) Percentage of total cells transfected with GFP-tail or GFP-stalk that exhibited compact perinuclear (yellow), perinuclear (blue), dispersed (red), or peripheral LE/lysosomes (green). Error bars, ±95% CI. *, $p \leq 0.0001$. (p values generated using Fisher's exact test for proportional data.) (E) Model of a role for Htt in coordinating organelle transport along the actin and microtubule cytoskeletons. In control cells, vesicular cargo, such as LE/lysosomes (green), are transported to the cell periphery along the microtubule (red) by kinesin-1 (purple) possibly via an adaptor complex involving HAP1 and Htt (yellow). There, they undergo a Htt-dependent change in cytoskeletal affinity, possibly via a myosin (brown) linker molecule such as optineurin. LE/lysosomes are able to return to the cell center by dynein-dependent microtubule transport (blue), facilitated by Htt. Under DHC RNAi conditions, LE/lysosomes can no longer undergo minus-end–directed microtubule transport and thus accumulate along the cell edge in the cortical actin network and are enmeshed in newly polymerized actin. In Htt RNAi cells, there is a decrease in new actin along the cell cortex, a defect in switching cytoskeletal tracks and inefficient dynein-mediated microtubule transport. As a result, LE/lysosomes do not concentrate at the perinuclear region and instead become more evenly distributed throughout the cytoplasm and accumulate at the microtubule plus-ends.

MATERIALS AND METHODS

Cells and immunocytochemistry

HeLa-M cells (a gift from Andrew Peden) were maintained in DMEM with glutamax and 10% fetal bovine serum. Cells grown on coverslips were fixed with 4% paraformaldehyde (PFA) and permeabilized with 0.2% saponin. Early endosomes were detected with either mouse monoclonal antibody (BD Transduction Laboratories, Lexington, KY) or rabbit polyclonal (Abcam, Boston, MA) to EEA1. Recycling and LE/lysosomes were detected with antibodies to Rab11 (rabbit polyclonal; Zymed, San Francisco, CA), or LAMP1 (rabbit polyclonal; Abcam). Antibodies to GFP (mouse monoclonal; Abcam), tubulin (DM1a; Sigma, St. Louis, MO), and cortactin (p80/85 mouse monoclonal; Millipore, Billerica, MA) were also used. Actin was stained with Alexa 594-phalloidin (Molecular Probes, Eugene, OR). Cells were incubated with Alexa fluorphore-conjugated secondary antibodies (Molecular Probes), and coverslips were mounted on slides using ProLong Gold antifade reagent (Invitrogen, Carlsbad, CA).

Plasmids and transfections

Htt1472 was constructed by introducing a termination codon at aa1472 into the mouse Htt sequence obtained from plasmid HU3 (a gift from Yvon Trottier) and then subcloning the truncation into pCDNA3 for mammalian expression. pcDNA1-Htt480 and full-length Htt (HD17) were gifts from Sandrine Humbert and Frederic Saudou; GFP-KIF5C tail and GFP-KIF5C stalk were gifts from Yoshiyuki Konishi and Mitsutoshi Setou. All DNA transfections were performed with Fugene (Roche, Indianapolis, IN). For RNAi knockdown, cells were transfected with siRNA duplexes (Dharmacon) directed against human Htt (GenBank NM_00211): 5′-GAACUAUCCUCUGGACGUAUU; a scrambled control oligo: 5′-GGUGACUCUAAUACUCCGAUU; or dynein heavy chain (GenBank NM_001376): 5′-GAGAGGAGGUUAUGUUUAAUU at a final concentration of 2.5–10 nM using Lipofectamine RNAiMax (Invitrogen). siRNA and DNA double transfections were performed sequentially with siRNAs transfected first followed by DNA transfection 24 h later. Cells were fixed 48 h after DNA transfection.

Immunoblot analysis

For Western blotting to detect knockdown, cells were lysed in low-detergent lysis buffer (10 mM Tris-HCl, 25 mM NaCl, 5 mM EDTA, 0.25% Igepal CA-630; Sigma) with protease inhibitor cocktail (Sigma). Total protein was measured using the BCA protein assay kit (Pierce, Rockford, IL). Blots were probed with antibodies against: transferrin receptor (CD71; BD Pharmingen, San Diego, CA), Htt (2166; Chemicon, Billerica, MA), DHC (R325, Santa Cruz Biotechnology, Santa Cruz, CA), β−catenin (BD Transduction), EGFR (Upstate, Billerica, MA), and phospho-ERK (p-ERK) (p44/42; Cell Signaling Technology, Beverly, MA). Chemiluminescence was enhanced by SuperSignal West Pico Chemiluminscent Sustrate (Thermo Scientific, Rochester, NY) and exposed to film or the Image Reader LAS-3000 (FUJIFILM Medical Systems USA, Stamford, CT). Densitometry was performed with Image-J (NIH, Rockville, MD).

Transferrin receptor uptake

To measure uptake from the plasma membrane, cells were lifted off plates by adding 5 mM EDTA in phosphate-buffered saline (PBS) and incubating at 37°C for 5 min. Cells were pelleted, resuspended in cold DMEM containing 25 mM HEPES and 10% fetal bovine serum (FBS) and anti-CD71 antibody diluted at 1:200, and incubated on ice for 30 min. Cells were washed twice with cold media and then incubated at 37°C for 0, 1, 2, 5, 15, and 30 min. Alexa-488 secondary antibody was diluted 1:200 into tubes, and cells were incubated on ice for 30 min. Cells were washed extensively, fixed in 4% PFA, resuspended in FACS buffer (5% FBS, 1 mM EDTA, 0.02% NaN_4 in PBS), and analyzed by flow cytometry (EPICS XL; Beckman Coulter, Brea, CA).

Transferrin trafficking assays

To label early endosomes, cells grown on coverslips were serum-starved for 40–50 min in DMEM containing 25 mM HEPES. Cells were bathed in DMEM containing 25 mM HEPES, 0.1% bovine serum albumin (BSA), and 50 μg/ml Alexa 594-Tf for 3 min at 37°C, then washed with warmed media containing 25 mM HEPES and 10% FBS, and incubated at 37°C for 12 min (including wash time). Cells were immediately fixed and processed for immunocytochemistry. To label recycling endosomes, cells were serum-starved as in the early endosome labeling and bathed in DMEM containing 25 mM HEPES, 0.1% BSA, and 50 μg/ml Alexa 594-Tf for 30 min at 37°C. Cells were washed in ice-cold media containing 25 mM HEPES and 10% FBS, transferred to warmed media for 0, 2, 5, 10, 20, or 60 min, washed with ice-cold PBS, and fixed immediately. To label recycling compartments for analysis by flow cytometry, cells were lifted off plates with 5 mM EDTA in PBS, pelleted, and resuspended in serum-free media containing 25 mM HEPES to serum starve for 30–40 min at 37°C. Cells were then pelleted and resuspended in DMEM containing 25 mM HEPES, 0.1% BSA, Tf-488 (50 μg/ml), and incubated at 37°C for 30 min. Cells were washed and resuspended in with ice-cold media containing 10% FBS and 25 mM HEPES, then transferred to 37°C for 0, 1, 2, 5, 10, 20, or 60 min, washed with ice-cold media, and fixed and prepared for flow cytometry as written above.

EGFR degradation

To measure EGFR degradation and p-ERK1/2 activation, cells were treated as previously reported (Taub *et al.*, 2007). Briefly, cells were serum starved for 14 h, stimulated with 100 ng/ml EGF (Sigma) for the indicated times, washed extensively, lysed in buffer containing protease and phosphatase inhibitors, and analyzed by Western blot.

Drug treatment

HeLa-M cells were treated with the indicated siRNAs for 48 h and then treated with 2 μM Latrunculin B (A.G. Scientific, San Diego, CA) or DMSO vehicle for 30 min, fixed in 4% PFA and stained for LAMP-1, F-actin, and microtubules. Images of at least 50 cells per condition were obtained at 63× using epifluorescence. Cells were scored for the number of LAMP-1-positive patches at the cell periphery. Phalloidin staining was used to assess the effects of Latrunculin B on the depolymerization of major stress fibers. Microtubules were not noticeably disrupted by Latrunculin B treatment.

Microscopy and quantitative analysis

Images were captured either as previously described (Levy *et al.*, 2006) or using a DMI6000 microscope with a 63× objective using Leica Application Suite for Advanced Fluorescence 2.1.2 (Leica Microsystems, Bannockburn, IL) and a charged-coupled device camera (Orca R2; Hamamatsu, Malvern, PA).

For linescans of LAMP1 intensity, line profiles, derived from a line bisecting the nucleus of each cell, were generated using Image-J (NIH). For analysis of early endosomes pulsed with Alexa-Tf, Z-series were obtained at 1-μm intervals, images were deconvolved, and the linescan of the maximum projection was generated with Leica MM Basic Offline Version 1.2 (Leica). For linescan analysis, fluorescence intensity along each line was interpolated to equalize the number of data points per line. Linescan intensities were normalized in two steps: first, each individual linescan was divided by its own median,

and second, all intensities were divided by the maximum intensity. The normalized linescans were averaged to generate a mean fluorescence intensity profile for each group of RNAi-treated cells. To evaluate the fluorescence intensity of exogenous Htt expression, transfected cells processed for immunocytochemistry with antibody against Htt were imaged at identical exposure times, and the sum of intensity values in a transfected cell (arbitrary units, a.u.) was divided by the area of the cell, measured using Leica MM Basic Offline Version 1.2 (Leica). High expressors had an intensity greater than or equal to ~1.7×10^4 a.u./μm^2, whereas cells with intensities below 1.7×10^4 a.u./μm^2 were considered as medium/low expressors. Colocalization and ROI measurements were performed using either LASAF6000 or MetaMorph software.

For analysis of lysosomal motility, cells were treated with the indicated siRNA oligos for 48 h and then incubated with LysoTracker Red (Molecular Probes) at a 1:1000 dilution for 1 min. Cells were imaged at 63× using epifluorescence at one frame per 2 s over 3 min. To measure lysosomal area, rolling ball background subtraction was performed on each frame, then maximum intensity projections were generated; images were thresholded with the Otsu function of ImageJ. The ratio of the resulting binary images of the first frame and the maximum intensity projection were used to estimate the extent of lysosomal motility. This displacement index describes the area the LE/lysosomes explore over the time course, with increased overlap a measure of decreased motility (Quintero *et al.*, 2009).

ACKNOWLEDGMENTS

We would like express our gratitude to Jeffrey Faust, Daniel Hussey, and David Ambrose of the Wistar Institute Flow Cytometry Facility for all their help. We are grateful to Mickey Marks, Subba Rao Ghangi Setty, and Margaret Chou for reagents and protocols for trafficking assays. We thank Eugen Buehler for statistical analysis and Sandra Maday, Eran Perlson, and Meng-meng Fu for critically reading the manuscript. This work was supported by the National Institutes of Health (GM48661 to E.L.F.H.).

REFERENCES

Aridor M, Hannan LA (2000). Traffic jam: a compendium of human diseases that affect intracellular transport processes. Traffic 1, 836–851.

Aridor M, Hannan LA (2002). Traffic jams II: an update of diseases of intracellular transport. Traffic 3, 781–790.

Atwal RS, Xia J, Pinchev D, Taylor J, Epand RM, Truant R (2007). Huntingtin has a membrane association signal that can modulate huntingtin aggregation, nuclear entry and toxicity. Hum Mol Genet 16, 2600–2615.

Brown CL, Maier KC, Stauber T, Ginkel LM, Wordeman L, Vernos I, Schroer TA (2005). Kinesin-2 is a motor for late endosomes and lysosomes. Traffic 6, 1114–1124.

Burkhardt JK, Echeverri CJ, Nilsson T, Vallee RBį (1997). Overexpression of the dynamitin (p50) subunit of the dynactin complex disrupts dynein-dependent maintenance of membrane organelle distribution. J Cell Biol 139, 469–484.

Caviston JP, Holzbaur EL (2006). Microtubule motors at the intersection of trafficking and transport. Trends Cell Biol 16, 530–537.

Caviston JP, Holzbaur EL (2009). Huntingtin as an essential integrator of intracellular vesicular trafficking. Trends Cell Biol 19, 147–155.

Caviston JP, Ross JL, Antony SM, Tokito M, Holzbaur EL (2007). Huntingtin facilitates dynein/dynactin-mediated vesicle transport. Proc Natl Acad Sci USA 104, 10045–10050.

Chevalier-Larsen E, Holzbaur EL (2006). Axonal transport and neurodegenerative disease. Biochim Biophys Acta 1762, 1094–1108.

Cole NB, Sciaky N, Marotta A, Song J, Lippincott-Schwartz J (1996). Golgi dispersal during microtubule disruption: regeneration of Golgi stacks at peripheral endoplasmic reticulum exit sites. Mol Biol Cell 7, 631–650.

Colin E, Zala D, Liot G, Rangone H, Borrell-Pages M, Li XJ, Saudou F, Humbert S (2008). Huntingtin phosphorylation acts as a molecular switch for anterograde/retrograde transport in neurons. EMBO J 27, 2124–2134.

Cordonnier MN, Dauzonne D, Louvard D, Coudrier E (2001). Actin filaments and myosin I alpha cooperate with microtubules for the movement of lysosomes. Mol Biol Cell 12, 4013–4029.

del Toro D, Alberch J, Lazaro-Dieguez F, Martin-Ibanez R, Xifro X, Egea G, Canals JM (2009). Mutant huntingtin impairs post-Golgi trafficking to lysosomes by delocalizing optineurin/Rab8 complex from the Golgi apparatus. Mol Biol Cell 20, 1478–1492.

Dell'Angelica EC (2009). AP-3-dependent trafficking and disease: the first decade. Curr Opin Cell Biol 21, 552–559.

DiFiglia M *et al.* (1995). Huntingtin is a cytoplasmic protein associated with vesicles in human and rat brain neurons. Neuron 14, 1075–1081.

Driskell OJ, Mironov A, Allan VJ, Woodman PG (2007). Dynein is required for receptor sorting and the morphogenesis of early endosomes. Nat Cell Biol 9, 113–120.

Engelender S, Sharp AH, Colomer V, Tokito MK, Lanahan A, Worley P, Holzbaur EL, Ross CA (1997). Huntingtin-associated protein 1 (HAP1) interacts with the p150Glued subunit of dynactin. Hum Mol Genet 6, 2205–2212.

Gauthier LR *et al.* (2004). Huntingtin controls neurotrophic support and survival of neurons by enhancing BDNF vesicular transport along microtubules. Cell 118, 127–138.

Harada A, Takei Y, Kanai Y, Tanaka Y, Nonaka S, Hirokawa N (1998). Golgi vesiculation and lysosome dispersion in cells lacking cytoplasmic dynein. J Cell Biol 141, 51–59.

Harjes P, Wanker EE (2003). The hunt for huntingtin function: interaction partners tell many different stories. Trends Biochem Sci 28, 425–433.

Hendricks AG, Perlson E, Ross JL, Schroeder HW 3rd, Tokito M, Holzbaur EL (2010). Motor coordination via a tug-of-war mechanism drives bidirectional vesicle transport. Curr Biol 20, 697–702.

Her LS, Goldstein LS (2008). Enhanced sensitivity of striatal neurons to axonal transport defects induced by mutant huntingtin. J Neurosci 28, 13662–13672.

Hilditch-Maguire P, Trettel F, Passani LA, Auerbach A, Persichetti F, MacDonald ME (2000). Huntingtin: an iron-regulated protein essential for normal nuclear and perinuclear organelles. Hum Mol Genet 9, 2789–2797.

Kegel KB *et al.* (2005). Huntingtin associates with acidic phospholipids at the plasma membrane. J Biol Chem 280, 36464–36473.

Konishi Y, Setou M (2009). Tubulin tyrosination navigates the kinesin-1 motor domain to axons. Nat Neurosci 12, 559–567.

Levy JR *et al.* (2006). A motor neuron disease-associated mutation in p150Glued perturbs dynactin function and induces protein aggregation. J Cell Biol 172, 733–745.

Li SH, Gutekunst CA, Hersch SM, Li XJ (1998). Interaction of huntingtin-associated protein with dynactin P150Glued. J Neurosci 18, 1261–1269.

Li SH, Li XJ (2004). Huntingtin-protein interactions and the pathogenesis of Huntington's disease. Trends Genet 20, 146–154.

Li X *et al.* (2009). Disruption of Rab11 activity in a knock-in mouse model of Huntington's disease. Neurobiol Dis 36, 374–383.

Loubery S, Wilhelm C, Hurbain I, Neveu S, Louvard D, Coudrier E (2008). Different microtubule motors move early and late endocytic compartments. Traffic 9, 492–509.

Lumsden AL, Henshall TL, Dayan S, Lardelli MT, Richards RI (2007). Huntingtin-deficient zebrafish exhibit defects in iron utilization and development. Hum Mol Genet 16, 1905–1920.

MacDonald ME (2003). Huntingtin: alive and well and working in middle management. Sci STKE 2003, pe48.

Maxfield FR, McGraw TE (2004). Endocytic recycling. Nat Rev Mol Cell Biol 5, 121–132.

McGuire JR, Rong J, Li SH, Li XJ (2006). Interaction of huntingtin-associated protein-1 with kinesin light chain: implications in intracellular trafficking in neurons. J Biol Chem 281, 3552–3559.

Pal A, Severin F, Lommer B, Shevchenko A, Zerial M (2006). Huntingtin-HAP40 complex is a novel Rab5 effector that regulates early endosome motility and is up-regulated in Huntington's disease. J Cell Biol 172, 605–618.

Palmer KJ, Hughes H, Stephens DJ (2009). Specificity of cytoplasmic dynein subunits in discrete membrane-trafficking steps. Mol Biol Cell 20, 2885–2899.

Quintero OA *et al.* (2009). Human Myo19 is a novel myosin that associates with mitochondria. Curr Biol 19, 2008–2013.

Sahlender DA, Roberts RC, Arden SD, Spudich G, Taylor MJ, Luzio JP, Kendrick-Jones J, Buss F (2005). Optineurin links myosin VI to the Golgi complex and is involved in Golgi organization and exocytosis. J Cell Biol 169, 285–295.

Saudou F, Finkbeiner S, Devys D, Greenberg ME (1998). Huntingtin acts in the nucleus to induce apoptosis but death does not correlate with the formation of intranuclear inclusions. Cell 95, 55–66.
Schroeder HW 3rd, Mitchell C, Shuman H, Holzbaur EL, Goldman YE (2010). Motor number controls cargo switching at actin-microtubule intersections in vitro. Curr Biol 20, 687–696.
Soldati T, Schliwa M (2006). Powering membrane traffic in endocytosis and recycling. Nat Rev Mol Cell Biol 7, 897–908.
Taub N, Teis D, Ebner HL, Hess MW, Huber LA (2007). Late endosomal traffic of the epidermal growth factor receptor ensures spatial and temporal fidelity of mitogen-activated protein kinase signaling. Mol Biol Cell 18, 4698–4710.
Taunton J, Rowning BA, Coughlin ML, Wu M, Moon RT, Mitchison TJ, Larabell CA (2000). Actin-dependent propulsion of endosomes and lysosomes by recruitment of N-WASP. J Cell Biol 148, 519–530.
The Huntington's Disease Collaborative Research Group (1993). A novel gene containing a trinucleotide repeat that is expanded and unstable on Huntington's disease chromosomes. Cell 72, 971–983.
Traer CJ, Rutherford AC, Palmer KJ, Wassmer T, Oakley J, Attar N, Carlton JG, Kremerskothen J, Stephens DJ, Cullen PJ (2007). SNX4 coordinates endosomal sorting of TfnR with dynein-mediated transport into the endocytic recycling compartment. Nat Cell Biol 9, 1370–1380.
Truant R, Atwal R, Burtnik A (2006). Hypothesis: Huntingtin may function in membrane association and vesicular trafficking. Biochem Cell Biol 84, 912–917.
Trushina E *et al.* (2004). Mutant huntingtin impairs axonal trafficking in mammalian neurons in vivo and in vitro. Mol Cell Biol 24, 8195–8209.
Twelvetrees AE *et al*. (2010). Delivery of GABAARs to synapses is mediated by HAP1-KIF5 and disrupted by mutant huntingtin. Neuron 65, 53–65.
Uruno T, Liu J, Zhang P, Fan Y, Egile C, Li R, Mueller SC, Zhan X (2001). Activation of Arp2/3 complex-mediated actin polymerization by cortactin. Nat Cell Biol 3, 259–266.
Valetti C, Wetzel DM, Schrader M, Hasbani MJ, Gill SR, Kreis TE, Schroer TA (1999). Role of dynactin in endocytic traffic: effects of dynamitin overexpression and colocalization with CLIP-170. Mol Biol Cell 10, 4107–4120.
Vincent C, Maridonneau-Parini I, Le Clainche C, Gounon P, Labrousse A (2007). Activation of p61Hck triggers WASp- and Arp2/3-dependent actin-comet tail biogenesis and accelerates lysosomes. J Biol Chem 282, 19565–19574.